Applied Optics, 1998, Vol. 37, Issue 31, pp. 7320-7326

Photothermal detection of trace optical absorption in water using visible light emitting diodes

Jane Hodgkinson[1,2,3], Mark Johnson[1] and John P Dakin[2]

1 North West Water Ltd, Dawson House, Great Sankey, Warrington, WA5 3LW, UK

2 Optoelectronics Research Centre, University of Southampton, Highfield, Southampton, SO17 1BJ, UK

3 Now at BG Technology, Gas R&T Centre, Ashby Rd, Loughborough, Leics, LE11 3GR, UK

Abstract

Visible light emitting diodes of three different colors have been used to detect an absorbing compound (potassium permanganate) in trace quantities in aqueous solution. Photothermal absorption in a closed cell caused deflection of a water meniscus held at a small pinhole. The displacement was monitored using optical fiber interferometry. The technique was limited by LED emission intensities and environmental acoustic noise, giving minimum detectable absorption coefficients of 2×10^{-4} cm^{-1} at 478 nm and 658 nm, and 3×10^{-4} cm^{-1} at 524 nm. The magnitude and form of meniscus deflection signals were shown to be in good agreement with theory.

1 Introduction

The measurement of optical absorption in water is a well-known analytical technique, used to determine the concentration of a dissolved absorbing compound. Water has a transmission window in the visible and ultraviolet, enabling spectroscopic determination of a number of compounds. Measurands of interest include residual chlorine, the visible color of the water (for aesthetic quality) and the general level of organic compounds (total organic carbon). Many detectors of metal ions and some recently developed pH meters use colorimetric methods involving reactive dyes. Potassium permanganate, chosen for this work as a representative absorption standard, is also sometimes used for disinfection of treated water.

Photothermal detection of trace chemicals in water has a number of advantages over conventional transmission spectroscopy, chiefly a high signal to noise ratio and relative insensitivity to light scattering within the sample [1,2]. However, much recent work has involved the use of high power cw or pulsed lasers,

the latter to remove window noise by time gating the signal [3]. The use of light emitting diodes (LEDs) as low-cost, reliable light sources has so far been restricted to solid samples[4,5] and gases[6]. These sources may be electronically modulated over a wide range of frequencies, avoiding the additional acoustic noise at the modulation frequency which would be expected when using a mechanical chopper. In this paper we report, as an example, the photothermal detection of potassium permanganate ($KMnO_4$) in aqueous solution using three visible LEDs.

2 Experimental

A novel closed-cell photothermal detector has been designed, suitable for measurement of aqueous samples using low power, cw light sources. The system has been described in greater detail[7], but the essential characteristics are presented here. The stainless steel cell had a cylindrical internal bore of length 50mm and radius 10mm. A flat, horizontal water meniscus was employed as a sensor, constrained by surface forces at a 200μm radius pinhole in nickel foil. Photothermal absorption of modulated light resulted in periodic pressure changes in the cell, which caused the meniscus to be deflected like a thin diaphragm, its curvature varying with the excess pressure in the cell. Vertical movement of the centre of the meniscus was detected using fiber optic interferometry. A schematic diagram of the apparatus is shown in Figure 1.

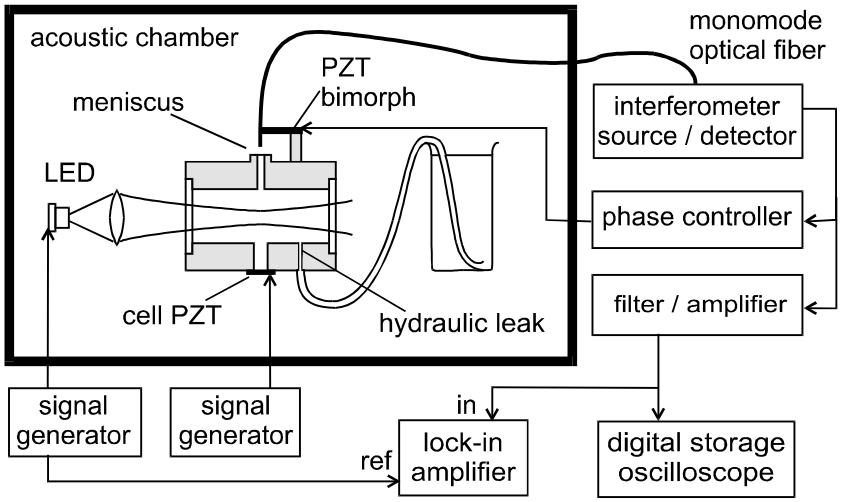

Figure 1. Schematic diagram of the system used for photothermal detection.

Zero mean pressure difference across the meniscus was maintained by a slow hydraulic leak to an outside reservoir, which equalised internal and external pressures at frequencies of less than ~5Hz, much lower than the photothermal modulation frequency. This arrangement kept the meniscus approximately flat, with small deflections from the mean position. An expanded view of the 400μm diameter meniscus and the

125μm diameter cleaved optical fiber end, which together formed the interferometer cavity, is shown in Figure 2. A distance of approximately 60μm was maintained between the two, to prevent accidental contact. While this reduced the coupling efficiency of the reflected light into the fiber, the sensitivity of the photothermal measurements was not affected.

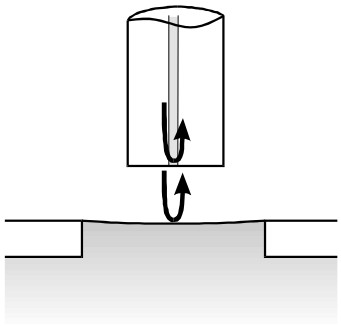

Figure 2. Interferometer formed by the cleaved optical fiber and the meniscus.

The full interferometer system is shown in Figure 3. Phase quadrature was maintained in the interferometer using a piezoelectric bimorph element (Quantelec EB-T-320), which moved the cleaved fiber end in relation to the meniscus. A feedback control circuit maintained a predetermined dc output from the interferometer receiver by applying a variable voltage to the bimorph, thus mechanically tracking an interference fringe edge. The photodiode at (2) was connected to a transimpedance amplifier, giving a voltage signal v which was converted to a displacement d using the formula;

$$\delta \mathrm{d} = \delta \mathrm{v} \ . \ \frac{\lambda}{4\pi A} \tag{1}$$

The value of the scale factor *A* (in volts) was determined by observation of the full-height fringes formed by large changes of optical phase.

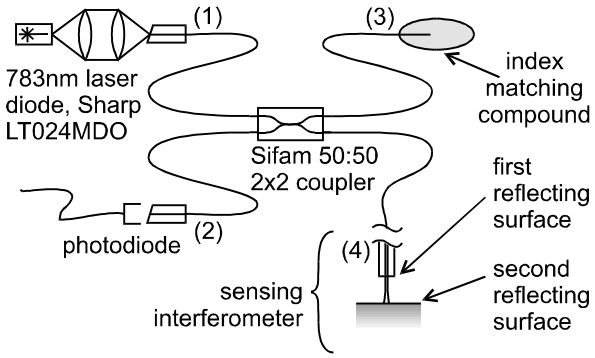

Figure 3. Low finesse fiber Fabry-Perot interferometer, used to detect the relative position of the meniscus.

The interferometer was used to measure the relative meniscus displacement with an rms noise floor at 70 Hz of 10 pm $Hz^{-1/2}$, which was a factor of 10 above the noise floor of an interferometer formed by the same cleaved fiber end and a firmly bonded silica test plate. This implies that the noise floor was due to random deflections of the meniscus itself, believed to be a result of environmental acoustic noise.

A piezoelectric element on the side of the cell, made of lead zirconate titanate (PZT) was used to modulate the cell volume for test purposes (Morgan Matroc PZT-5A, 0.48mm thick, 10mm square, bonded to a 6mm diameter hole in the cell wall). Applying a voltage across the cell PZT resulted in a large meniscus deflection, whose magnitude was proportional to the applied voltage.

The plastic lens on the front of each LED was polished flat, as close as possible to the LED chip itself. The back and sides of each package were painted black to reduce stray light. Otherwise, spurious signals could have resulted from stray light hitting and being absorbed by the cell walls. The light output was coupled into the photothermal cell using an f/3.2 lens. Each LED was driven using a square-wave voltage from a signal generator (Thurlby Thandar TG220) with a 220Ω resistor in series to give a peak drive current of 30mA. 70Hz was chosen as the preferred modulation frequency because the measurement signal to noise ratio was a maximum at this frequency. Signals from the interferometer were passed through a high pass filter / amplifier (EG&G model 5113, amplification ×10 for frequencies > 1Hz, 12 dB / decade roll-off filter for lower frequencies). A lock-in amplifier (EG&G model 5210) in R, θ mode with a 100s integration time was used to detect signals synchronous with the modulation. A digital storage oscilloscope (Hitachi VC-6175) was used to record the shapes of photothermal signals.

LED emission intensity was measured using a large area silicon photodiode (Centronic OST100/7CQ) in the position normally occupied by the cell. The photodiode current was related to the incident light intensity, using the manufacturer's quoted responsivity at each wavelength with an estimated absolute error of 15%. The quoted responsivity at 780nm was checked using a commercial fiber optic power meter (Megger OTP 510, also incorporating a silicon photodiode).

The measured peak-to-peak modulated light intensities and peak absorbed wavelengths of each LED are shown in Table 1. The peak absorbed wavelength may be displaced slightly from the peak emitted wavelength because of the shape of the permanganate absorption spectrum. For the purpose of estimating the magnitude of the photothermal signal, it was assumed that the LED emission was all at the peak absorbed wavelength.

Table 1. Measured emission of the three LEDs used for photothermal detection.

	Intensity / mW	Wavelength	Reference
Blue	0.75±0.11	478 nm	Marl 110106
Green	0.50±0.08	524 nm	Marl 110104
Red	0.88±0.13	658 nm	LED Technology LURR3000G3

The relative emission spectrum from each LED each is shown in Figure 4, with the absorption spectrum for potassium permanganate in solution, determined using a diode array spectrometer (HP 8452A) with a 4cm pathlength cell against a deionised water blank. $KMnO_4$ is known to be a good standard for use as a photothermal absorber, because it doesn't fluoresce, phosphoresce or undergo photochemical reactions when excited in the visible, and therefore delivers absorbed energy quickly to the solvent as heat[8].

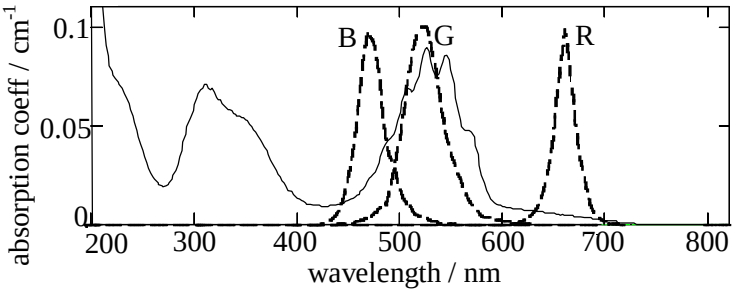

Figure 4. Absorption spectrum of 5ppm $KMnO_4$ in solution (solid line), with the normalized emission spectra of blue, green and red LEDs superimposed (dashed lines) all determined using a diode array spectrometer.

$KMnO_4$ solutions were prepared by dilution of a known quantity of the solid. Signals from a range of solutions strengths were recorded for excitation by each LED. The diode array spectrometer was used to measure the absorption of $KMnO_4$ in each sample, at each of the LED peak wavelengths. The five weakest solutions had too low an absorption coefficient at 478nm and 658nm to be accurately measured in this way, so the absorption was calculated by reference to that measured at 530nm, corresponding to an absorption peak.

The experimental procedure was as follows. The cell was filled with a test solution and the interferometer aligned by eye to the center of the meniscus using an xyz stage. A sinusoidal voltage of approximately 10V peak-to-peak was applied to the cell PZT in order to modulate the cell volume. The resulting periodic meniscus displacement produced interference fringes which were used to align the fiber more precisely to the position of maximum meniscus movement. The interference fringes were also used to determine the correct quadrature setpoint for the phase controller.

Two scale factors were recorded for each measurement, namely the interference fringe depth and the voltage required, across the cell PZT, to move the meniscus by two interference fringes (783nm). The latter provided an approximate measure of the response of the system to a given volume change and proved useful in detecting the undesirable presence of large air bubbles in the cell, which would have reduced the signal. It would also account for any changes in the surface tension of the water at the meniscus, due for example to the presence of impurities such as surfactants. Finally, the sinusoidal voltage across the cell PZT was removed and the system was ready to make measurements.

Photothermal signals have a strong temperature dependence in water, which was expected to be approximately linear over our working range (20-25°C), falling to zero at 4EC [1]. The ambient temperature was measured during each measurement. It was assumed that the $KMnO_4$ solutions had reached thermal equilibrium with the surroundings, and that any temperature increase during each measurement was negligible.

The voltage measurements were converted to a meniscus displacement in nm, using the measured fringe depth and assuming that phase quadrature was maintained. The results were further normalized for differences in ambient temperature and in the cell responsivity, as measured by finding the voltage applied across the cell PZT which was required to move the meniscus by a known distance.

3 Results and discussion

3.1 Magnitude and form of photothermal signals

The green LED, whose emission corresponded approximately to an absorption maximum of $KMnO_4$, was used with a strongly absorbing solution to investigate the frequency response of the system and the form and magnitude of photothermal signals. The shape and magnitude of the modulated emission waveform from the LED were found to be constant over the frequency range of these experiments. The shapes of the

photothermal signals at various frequencies were recorded using the digital storage oscilloscope as averages over 256 traces, and are shown in Figure 5.

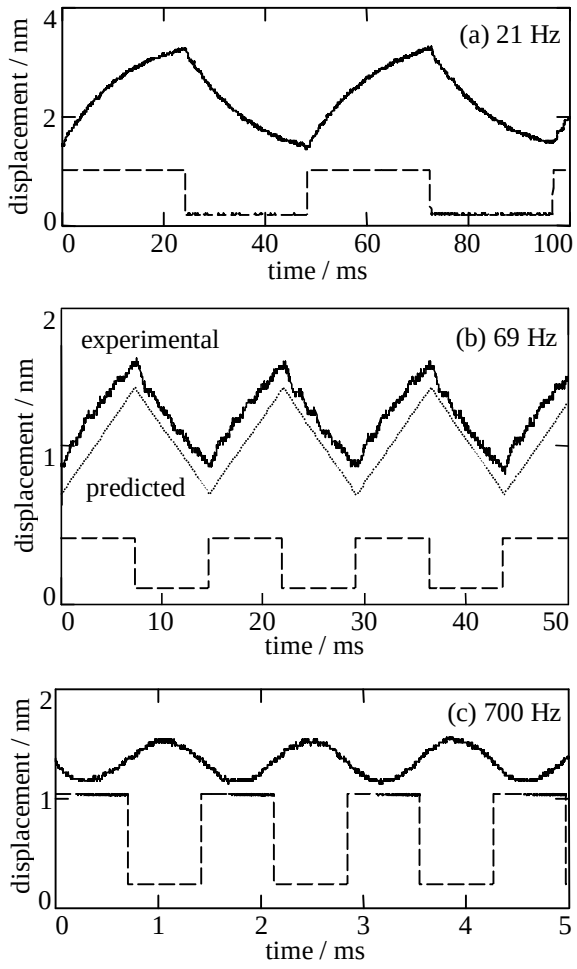

Figure 5. Photothermal signals resulting from absorption of light from a green LED in a 50ppm solution of $KMnO_4$.

The expected shape and size of the meniscus displacement, for a given energy input, have been calculated in the Appendix. For a $KMnO_4$ concentration of 3×10^{-4} M, it was expected that over 99.7% of the light would be absorbed, over the fwhm range of LED emission. A sawtooth meniscus deflection was predicted by equation (7) for square wave excitation, giving a displacement per unit absorbed energy of $\Delta h = 4\times10^{-4}$ m J^{-1}. The predicted photothermal signal has been calculated from the measured LED emission, with an estimated error of 15%. That and the actual signal recorded by a digital storage oscilloscope (averaged over 256 traces) are shown in Figure 5 (b). They are in good agreement.

The frequency response of photothermal signals, from the same solution, is shown in Figure 6. For photothermal signals, a 1/f response is predicted. The results are in good agreement with this, except for a distinct resonance observed at 700Hz. There was no observed gain in signal to noise ratio associated with modulation at 700Hz, because the noise level was also increased at the resonant frequency. The precise origin of the resonance was not determined, but it was experimentally confirmed to be associated with the water meniscus, the water in the cell and the cell PZT.

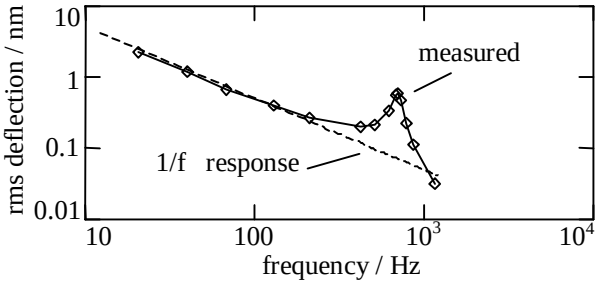

Figure 6. Frequency response for photothermal signals produced when modulated light from a green LED was absorbed by a 50ppm solution of $KMnO_4$.

The resonant signal in Figure 5 (c) is clearly different from that of the lower frequency signals, in that it is sinusoidal and has undergone a phase shift of approximately -90° with respect to the lower frequency signals. The same resonance can also be seen, at lower frequency modulation, as a small ripple in Figure 5 (b). The form of Figure 5 (a) indicates a degree of high pass filtering, with a time constant of the order of 20ms, which is too small to have been caused by either the hydraulic leak, the phase controller, or the high pass filters used on both the oscilloscope and the EG&G filter / amplifier. However, the combination of all four filters could have created an effective 3dB cut-off at a higher frequency.

3.2 Detection of $KMnO_4$ in aqueous solution

The three LEDs, modulated at 70Hz, were each used to excite photothermal signals in a range of aqueous solutions of $KMnO_4$. The signals, converted to rms meniscus displacements, are shown in Figure 7 versus the absorption coefficients of the various levels of $KMnO_4$ in solution. Three types of behaviour were expected from equation (7). At very low concentrations of $KMnO_4$, the absorption of the water itself should dominate. Whether or not the presence of $KMnO_4$ can be determined depends on the repeatability of the photothermal measurement, because absorption changes smaller than the background water absorption can only be discerned by subtraction of a blank reference measurement for pure water. At intermediate absorptions the permanganate should dominate, and the photothermal signal should be proportional to the concentration of $KMnO_4$. At high concentrations, with values of α above $0.1cm^{-1}$ for a

5cm pathlength, a nonlinear dependence on α should emerge and the photothermal signal should converge to its maximum possible value. If the photothermal signal is plotted against the fraction of light absorbed, a linear dependence should be observed above the noise level, even at high $KMnO_4$ concentrations.

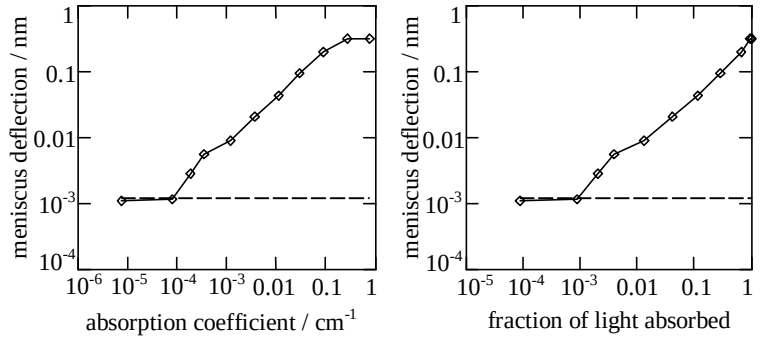

(a) Blue LED, 478nm

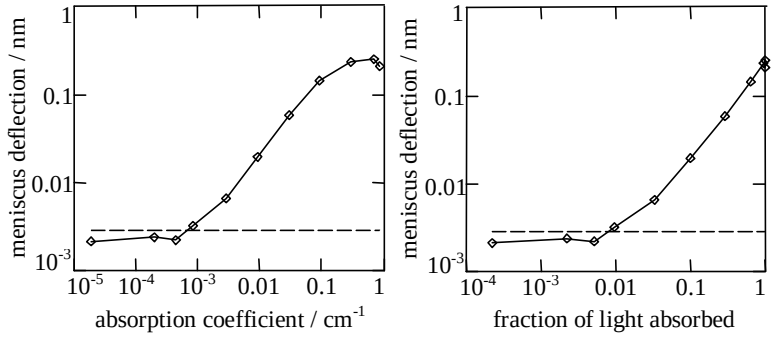

(b) Green LED, 524nm

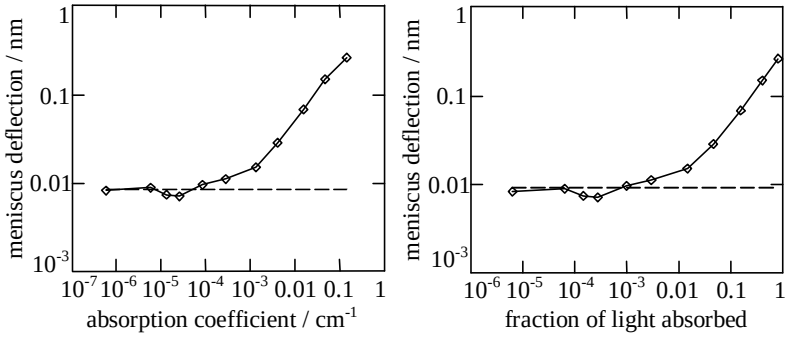

(c) Red LED, 658nm

Figure 7. Photothermal signals from $KMnO_4$ solutions (solid line) and from deionised water controls (dashed line), versus the absorption coefficients and fractional light absorption of $KMnO_4$ at each wavelength.

In each case the form of the graph is as expected, with an approximately linear increase in photothermal signal with absorption coefficient for values of α above that of water and below the point of saturation of

the signal. The main sources of error in the data were as follows. At low absorptions, random noise in the interferometer signal, estimated to be 10 pm $Hz^{-1/2}$, gave a 1pm random uncertainty in the results for a 100s measurement period. Secondly, interference fringe drift resulted in uncertainty in the value of the scale factor *A* used to calculate the meniscus deflections using equation (1). This produced an error of approximately 10% in each result.

The performance of our system in detecting trace levels of absorption in water depended on the photothermal modulation frequency (70Hz in each case), the limiting noise level, the light power coupled into the cell from the source and the background level of water absorption. The limiting noise was the minimum detectable meniscus deflection of 1pm. Equation (8) predicts the resulting minimum detectable absorption coefficients, which are given in Table 2, for each LED. Also shown is the expected background level of water absorption, as recorded by Patel and Tam using a pulsed photothermal method[3].

Table 2. Predicted photothermal performance with each LED

	Predicted α_{min}	Water absorption[3]
Blue LED	2×10^{-4} cm^{-1}	1.1×10^{-4} cm^{-1}
Green LED	3×10^{-4} cm^{-1}	1.4×10^{-4} cm^{-1}
Red LED	2×10^{-4} cm^{-1}	1.4×10^{-3} cm^{-1}

The graphical results are consistent with the predicted minimum detectable absorption levels for each LED. All three LEDs had similar output intensities, and so similar minimum detectable absorption levels were predicted. However, the absorption coefficient of water itself at 658nm is higher than the predicted minimum detectable α for the red LED. In this case, the predicted performance could only be achieved by arithmetic subtraction of the blank reference signal due to deionised water, as shown in Figure 8. An estimate of the measurement repeatability, the value of one standard deviation in the measured results for water, is shown as a dashed line.

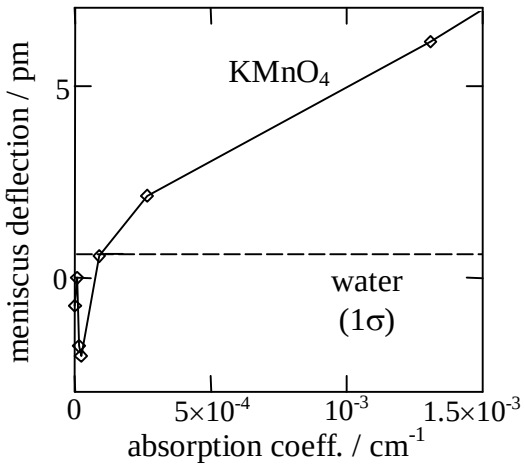

Figure 8. Photothermal meniscus deflection results excited by a 658nm LED, following subtraction of the mean measured meniscus deflection for a deionised water control.

Thus, for each of the three measurements of $KMnO_4$ concentration in deionised water, the meniscus deflection noise floor of 1 pm limits the minimum detectable absorption. The fact that this limit is determined by random displacement of the meniscus suggests that improvements may be gained by greater suppression of environmental acoustic noise. Alternatively, under some circumstances, longer measurement integration periods might be desirable. Photothermal window noise does not appear to have been significant, perhaps due to our choice of sapphire as the window material. Sapphire is reported to have thermal transfer properties which result in lower window noise levels than are produced using other common window materials, such as silica[1].

4 Conclusion

Photothermal detection of trace quantities of potassium permanganate in aqueous solution has been demonstrated, using three LEDs emitting visible light at different wavelengths. Potassium permanganate is a good photothermal standard, enabling our results to be transferred to other compounds. The system used a water meniscus as a pressure sensor, of optimum compliance approximately equal to the bulk compliance of the water enclosed by the cell. Meniscus deflections were detected using an optical fiber Fabry-Perot interferometer.

The technique was limited by environmental acoustic noise which gave a noise floor, in terms of rms meniscus displacement, of 10 pm $Hz^{-1/2}$. For a measurement integration time of 100s, this limit was equivalent to a minimum detectable absorbed power of 0.25 μW rms. The minimum detectable absorption

coefficient depended on the emitted power of the light sources; in our case the limit was of the order of 2×10^{-4} cm^{-1}.

The magnitude and shape of photothermal signals were found to be in good agreement with theory. The frequency response of the technique showed a 1/f relationship, with a resonance at approximately 700Hz. However, the resonance was not exploited during our experiments because the signal to noise ratio was not enhanced.

Acknowledgements

This work was supported by North West Water Ltd and the EPSRC / Department of Trade and Industry, through the UK Teaching Company Scheme.

References

1. A. Rosencwaig, *Photoacoustics and photoacoustic spectroscopy*. (Wiley, New York, 1980).
2. Y.-H. Pao, *Optoacoustic spectroscopy and detection* (Academic Press, New York, 1977).
3. C. K. N. Patel and A. C. Tam, "Pulsed optoacoustic spectroscopy of condensed matter," Rev. Mod. Phys. **53**, 517-550 (1981).
4. C. Saloma and A. J. de Vera, "Photoacoustic depth profiling by cross-correlation using a GaAs light emitting diode," Appl. Opt. **30**, 2393-2397 (1991).
5. C. Viappiani and G. Rivera, "Use of LEDs as light sources in photoacoustic spectroscopy," Meas. Sci. Tech. **1**, 1257-1259 (1990).
6. J. W. Chey, P. Sultan and H. J. Gerritsen, "Resonant photoacoustic detection of methane in nitrogen using a room temperature infrared light emitting diode," Appl. Opt. **26**, 3192-3194 (1987).
7. J. Hodgkinson, M. Johnson and J. P. Dakin. "Photothermal detection of trace compounds in water, using the deflection of a water meniscus," Meas. Sci. Tech. In press.
8. S. E. Braslavsky and G. E. Heibel, "Time-resolved photothermal and photoacoustic methods applied to photoinduced processes in solution," Chem. Rev. **92** 1381-1410 (1992).

Appendix –Theory of operation

The following assumptions have been made in order to calculate the deflection of the center of the meniscus, Δh, as a function of photothermally absorbed energy.

(i) The presence of impurities in the water, including the compound that we wish to detect, has a negligible effect on its material properties.
(ii) The light emitted by each LED is monochromatic at the peak absorbed wavelength.
(iii) All the light energy absorbed by the solution is converted to heat within the modulation period of the measurement, and during this period, no heat is lost from the fluid, for example to the cell walls.
(iv) A flat meniscus is used for detection purposes, with small deflections from this equilibrium.
(v) The edge of the pinhole is perfectly sharp (zero radius of curvature).
(vi) The curvature of the meniscus is constant across the pinhole, ie surface forces dominate gravity and deflections are spherical.

Firstly, the mechanical compliance of the cell is calculated, ie the change in volume caused by an internal pressure change. This is used to calculate the magnitude of the photothermal response, and the optimum value of the meniscus radius is found. Finally, the magnitude of the signal from the fiber optic interferometer is calculated.

The compliances (∂V/∂P) of different cell elements are additive, and may be considered one by one. The compliance of the water enclosed by the cell may be calculated from the definition of its bulk modulus κ and the internal volume of the cell V_c.

$$\left(\frac{\partial \mathrm{V}}{\partial \mathrm{P}}\right)_{\mathrm{water}} = \frac{V_c}{\kappa} \tag{2}$$

The compliance of the meniscus may be found by considering the excess pressure across the curved meniscus and by calculating the volume of displaced fluid. For small deflections from a flat surface, the meniscus compliance is approximately linear with respect to θ, and the expression converges to the following;

$$\left(\frac{\partial V}{\partial P}\right)_{\mathrm{meniscus}} = \frac{\pi a^4}{8\gamma} \tag{3}$$

where γ is the surface tension of the fluid. When a cylindrical region of fluid lying in the optical path absorbs a small amount of light energy δE, its unconstrained volume increase would be,

$$\delta V = \frac{\beta \ \delta E}{C_p \ \rho} \tag{4}$$

where β is the volume thermal expansion coefficient of the fluid, C_p is its specific heat capacity and ρ is its density. The pressure increase in a closed cell on absorption of energy δE is thus given by equation (4) and the total cell compliance.

The displacement of the center of the flat meniscus from its mean position, Δh, is a function of the excess pressure across it, which for small pressure changes approximates to the following linear expression;

$$\Delta h = \frac{a^2 \ \Delta P}{4 \gamma} \tag{5}$$

The change in Δh with absorbed energy E is then given by;

$$\frac{\partial \Delta h}{\partial E} = \frac{\beta \ a^2}{4 C_p \rho \gamma} \ \frac{1}{\left(\frac{V_c}{\kappa} + \frac{\pi a^4}{8 \gamma} \right)} \tag{6}$$

The optimum meniscus, for maximum displacement response to absorbed energy, has a radius which makes its compliance equal to the bulk compliance of the water enclosed by the cell. In this case, the optimum radius is 200μm[7], giving a response to absorbed energy of $\Delta h = 4 \times 10^{-4}$ m J^{-1}.

The absorbed energy is given by Beer's Law. For small absorption coefficients, E is approximately proportional to α, the absorption coefficient. For square wave modulation of the light at a frequency f, the absorbed energy takes the form of a sawtooth, plus a ramp component. Since our method subtracts the ramp component from the signal, we may ignore it. The meniscus deflection then simply takes the form of a sawtooth, with the peak-to-peak displacement given by the following equation;

$$\Delta h_{p-p} = \left(4 \times 10^{-4} \right) \ \frac{I_0}{2 \mathrm{f}} \ \left[1 - 10^{-\alpha(\lambda) \ell} \right] \tag{7}$$

where I_0 is the peak incident light power, $\alpha(\lambda)$ is the absorption coefficient, in cm^{-1} at a particular wavelength λ and ℓ is the pathlength of the cell in cm. For small Δh, the relationship between the minimum detectable absorption coefficient and the rms minimum detectable meniscus deflection is approximated by;

$$\alpha_{\min} \approx 10^4 \ \frac{\mathrm{f} \ \Delta h_{\mathrm{rms}}}{I_0 \ \ell} \tag{8}$$